Neuron, Vol. 24, 701–713, November, 1999, Copyright ©1999 by Cell Press

Facilitation of NMDAR-Independent LTP and Spatial Learning in Mutant Mice Lacking Ryanodine Receptor Type 3

Akira Futatsugi,[1,2,3,9] Kunio Kato,[3,8,9] Hiroo Ogura,[4] Sheng-Tian Li,[2,7] Eiichiro Nagata,[5] Goro Kuwajima,[1] Kortaro Tanaka,[5] Shigeyoshi Itohara,[6] and Katsuhiko Mikoshiba[2,3,7]

[1]Shionogi Institute for Medical Science
Shionogi and Company, Ltd.
2-5-1 Mishima, Settsu-shi
Osaka 566-0022
[2]Department of Molecular Neurobiology
Institute of Medical Science
University of Tokyo
4-6-1 Shirokanedai, Minato-ku
Tokyo 108-8639
[3]Mikoshiba Calciosignal Net Project
Exploratory Research for Advanced Technology
Japan Science and Technology Corporation
2-28-8 Honkomagome, Bunkyo-ku
Tokyo 113-0021
[4]Tsukuba Research Laboratories
Eisai Company, Ltd.
Tokodai, Tsukuba-shi
Ibaraki 300-2635
[5]Department of Neurology
School of Medicine
Keio University
35 Shinanomachi, Shinjuku-ku
Tokyo 160-8582
[6]Laboratory for Behavior Genetics
[7]Developmental Neurobiology Laboratory
Brain Science Institute
RIKEN
2-1 Hirosawa, Wako-shi
Saitama 351–0198
Japan

Summary

To evaluate the role in synaptic plasticity of ryanodine receptor type 3 (*RyR3*), which is normally enriched in hippocampal area CA1, we generated *RyR3*-deficient mice. Mutant mice exhibited facilitated CA1 long-term potentiation (LTP) induced by short tetanus (100 Hz, 100 ms) stimulation. Unlike LTP in wild-type mice, this LTP was not blocked by the NMDA receptor antagonist D-AP5 but was partially dependent on L-type voltage-dependent Ca^{2+} channels (VDCCs) and metabotropic glutamate receptors (mGluRs). Long-term depression (LTD) was not induced in *RyR3*-deficient mice. *RyR3*-deficient mice also exhibited improved spatial learning on a Morris water maze task. These results suggest that in wild-type mice, in contrast to the excitatory role of Ca^{2+} influx, *RyR3*-mediated intracellular Ca^{2+} ($[Ca^{2+}]_i$) release from endoplasmic reticulum (ER) may inhibit hippocampal LTP and spatial learning.

[8]To whom correspondence should be addressed (e-mail: kunio@ims.u-tokyo.ac.jp).
[9]These authors contributed equally to this work.

Introduction

Long-term potentiation (LTP) and long-term depression (LTD) are long-lasting changes in synaptic strength and are generally considered to be a cellular substrate for the encoding of memory (Dudek and Bear, 1992; Bliss and Collingridge, 1993). In particular, it has been suggested that LTP in pyramidal cells of the CA1 region of the hippocampus may be a primary synaptic mechanism underlying specific types of long-term memory, such as spatial and contextual learning (McHugh et al., 1996; Tsien et al., 1996). It is well established that the induction of LTP and LTD shares a common trigger step: an increase in intracellular Ca^{2+} ($[Ca^{2+}]_i$) (Lynch et al., 1983; Mulkey and Malenka, 1992) that is mediated primarily by the influx of Ca^{2+} through postsynaptic N-methyl-D-aspartate (NMDA) receptors (Collingridge, 1987; Dudek and Bear, 1992), although other Ca^{2+} sources may substitute under certain experimental conditions (Grover and Teyler, 1990; Kato et al., 1993; Jia et al., 1996). The production of LTP or LTD may also depend on the level of increase in $[Ca^{2+}]_i$ (Cummings et al., 1996). A number of studies have suggested that a large increase in postsynaptic Ca^{2+} activates protein kinases such as PKC and Ca^{2+}/calmodulin-dependent protein kinase (CaMK), which is present at high levels just below the postsynaptic membrane and contributes to the induction of LTP (Malenka et al., 1986; Abeliovich et al., 1993; Barria et al., 1997). On the other hand, LTD induction is selectively blocked by serine–threonine protein phosphatase inhibitors; therefore phosphatases, particularly calcineurin in the central nervous system, are likely to be primarily activated at a lower level of $[Ca^{2+}]_i$ increase, contributing to LTD induction (Mulkey et al., 1993, 1994). The mechanism underlying the production of LTP versus LTD remains unknown, however, and the role of Ca^{2+} release from intracellular stores on this regulation remains to be fully examined.

Two types of Ca^{2+} release localized on endoplasmic reticulum (ER) have been described: inositol 1,4,5-trisphosphate (IP_3) -induced Ca^{2+} release (IICR) and Ca^{2+}-induced Ca^{2+} release (CICR). IP_3 receptors (IP_3Rs) are activated by IP_3, which is primarily produced as a result of metabotropic glutamate receptor (mGluR) activation in the neuron. Glutamate is a major neurotransmitter in the brain, and IICR is thought to have a role in synaptic plasticity (Harvey and Collingridge, 1992; Inoue et al., 1998). CICR occurs via ryanodine-sensitive receptors (RyRs). RyRs consist of at least three subtypes of receptors: RyR1, RyR2, and *RyR3*. RyR1 and RyR2 are predominantly expressed in skeletal and cardiac muscle, while *RyR3* is enriched in specific areas in the brain, particularly the CA1 region of hippocampus (Furuichi et al., 1994; Giannini et al., 1995; Murayama and Ogawa, 1996). Results of studies of *RyR3* knockout mice (Bertocchini et al., 1997) indicate that although *RyR3* is not the major subtype expressed in skeletal muscle, it has a significant role, albeit supplemental to RyR1, in excitation–contraction coupling in skeletal muscle. Also using RyR1 and *RyR3* knockout mice, Takeshima et al. (1996)

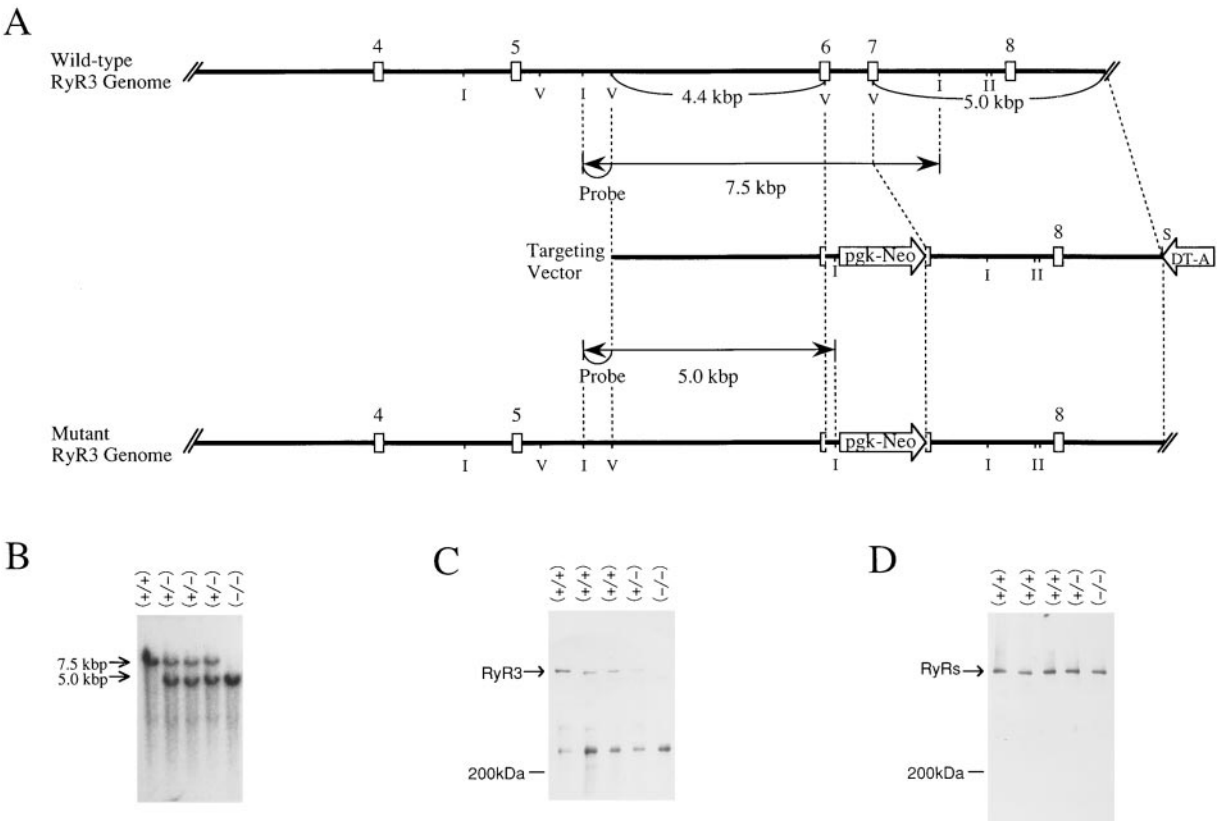

Figure 1. Generation of *RyR3*-Deficient Mice

(A) A schematic drawing of the targeting construct and part of the *RyR3* gene. Exons (open boxes) are numbered according to those of the human RyR1 gene. A 0.85 kb fragment from the EcoRV site in exon 6 to the EcoRV site in exon 7 was deleted and replaced with a *neo* gene. The probe used for screening the ES cell clones and mice is indicated. The targeting vector included a neomycin resistance gene driven by the PGK promoter (PGK-*neo*) and a diphtheria toxin A fragment gene (*DT-A*) driven by the MC1 promoter as positive and negative selection markers, respectively. Abbreviations: I, EcoRI; S, SalI; V, EcoRV.

(B) Southern blot analysis of genomic DNA isolated from mouse tail tissue. Genomic DNA was digested with EcoRI and probed with a 0.6 kb fragment 5′ to the exon that corresponds to exon 6 of human RyR1, yielding 7.5 kb restriction fragments from wild-type and 5.0 kb fragments from mutant alleles (see [A]). Wild-type and mutant alleles are indicated.

(C) Western blot analysis of *RyR3* expression in microsomal fractions of the cerebrum, including the hippocampus (5 μg) from wild-type (+/+), heterozygous (+/−), and homozygous (−/−) mice. The blot was probed with affinity-purified anti-B4 antibody.

(D) Western blot analysis of the expression of RyRs in microsomal fractions of cerebrum, including the hippocampus (5 μg) from wild-type (+/+), heterozygous (+/−), and homozygous (−/−) mice. The blot was probed with an affinity-purified anti-C2 antibody.

showed that *RyR3* has a lower sensitivity to $[Ca^{2+}]_i$ than RyR1 in skeletal muscle, suggesting that the functions of RyR1 and *RyR3* are subtly different.

Although Ca^{2+} influx is essential for the induction of LTP, it has been shown that the initial Ca^{2+} influx may be further amplified by CICR. The involvement of RyRs in synaptic plasticity has also been reported; however, the results from these studies appear to be contradictory, presumably due to differences in experimental conditions. Obenaus et al. (1989) indicated that dantrolene, an inhibitor of RyRs, blocks the induction of LTP in hippocampal dentate gyrus. O'Mara et al. (1995) suggested that dantrolene inhibits LTD and depotentiation in the CA1, while LTP was enhanced. Wang et al. (1996) reported that in the presence of ryanodine a low-frequency stimulation, which normally induces LTD, induces NMDA receptor–independent LTP.

The distribution of *RyR3* in the brain (Ellisman et al., 1990; Ouyang et al., 1993; Giannini et al., 1995), particularly its enrichment in hippocampal CA1 pyramidal neurons (Furuichi et al., 1994; Murayama and Ogawa, 1996), suggests a specialized role of these receptors in this area critical for memory formation. To conclusively determine the role of RyRs, especially *RyR3*-mediated changes in $[Ca^{2+}]_i$ in LTP and learning, we generated mice lacking *RyR3*. We measured the electrophysiological and pharmacological properties of synaptic plasticity in the CA1 area of the mutant mice and the performance of these animals in spatial learning tasks.

Results

Features of *RyR3* Knockout Mice

We generated mutant mice in which the *RyR3* gene was disrupted between the regions corresponding to exon 6 and exon 7 of human type 1 RyR (Phillips et al., 1996) and was replaced by a PGK-*neo* gene carrying stop codons in all the reading frames and a poly(A) tail (Figure 1A). The disrupted region was between the sites that correspond to Gly-145 and Glu-215 of rabbit *RyR3*. E14 embryonic stem (ES) cells were electroporated with the

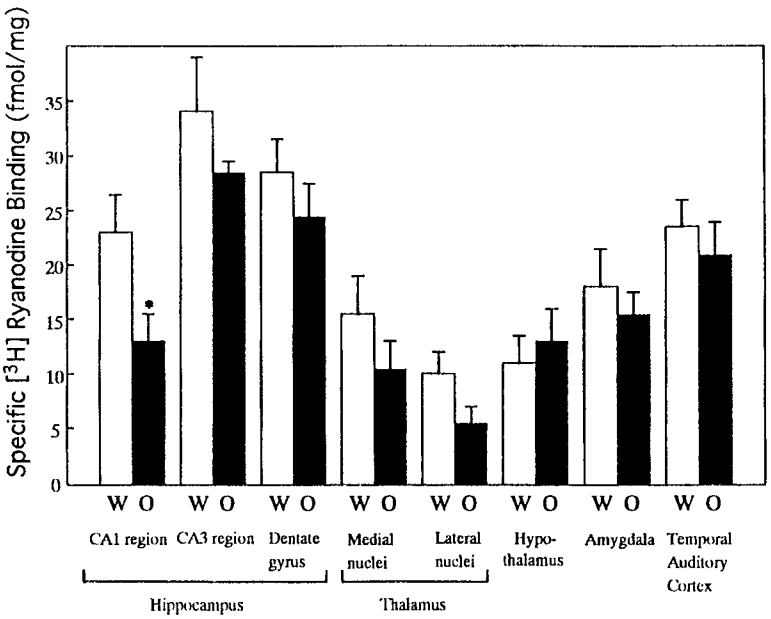

Figure 2. [^{3}H]Ryanodine Binding to Brain Sections

Specific [^{3}H]ryanodine binding to various areas of hippocampus–thalamus level sections from wild-type (+/+) and homozygous (−/−) mice. Only the CA1 region of the hippocampus from homozygous mice exhibited significant reductions in [^{3}H]ryanodine binding compared with that in wild-type littermates. Each vertical bar and line indicates the mean ± SEM (n = 10). Significant difference from wild type: *$p < 0.05$ (Student's t test). Abbreviations: W, wild type; O, homozygote.

targeting vector (Figure 1A) and were selected by positive–negative selection (Mansour et al., 1988). The selected clones were screened for the desired homologous recombination by Southern blot analysis using the 5′ external probe and the *neo* probe (data not shown). Two lines of *RyR3*-deficient mice, derived from two independent ES clones, were generated. They yielded essentially the same results in all the experiments described below. Southern blot analysis revealed clear patterns of gene disruption (Figure 1B). Cross-breeding between heterozygous mutants generated mice of each genotype (wild type, +/+, n = 195; heterozygotes, +/−, n = 395; and homozygotes, −/−, n = 191), suggesting that homozygotes exhibit normal embryonic development. After birth, homozygotes grew normally with no apparent change in viability up to at least 24 months. Homozygotes were fertile and were indistinguishable in appearance from wild-type and heterozygous littermates. These features were similar to those of independent *RyR3*-deficient mouse lines generated by Takeshima et al. (1996) and Bertocchini et al. (1997).

Immunoblot analysis of the microsomal fraction of the cerebrum, including the hippocampus, using a *RyR3*-specific antibody and an antibody that cross-reacts with all RyRs showed that the expression of *RyR3* was disrupted, whereas the expression of other subtypes of RyRs (RyR1 and RyR2) was not altered in the mutant mice (Figures 1C and 1D).

[^{3}H]Ryanodine binding was greatly reduced in the hippocampal CA1 region of the homozygotes (+/+ mice: 23.2 ± 3.2 fmol/mg, n = 10; −/− mice: 13.2 ± 2.1 fmol/mg, n = 10 [mean ± SEM]; Student's t test, $p < 0.05$; Figure 2). The residual [^{3}H]ryanodine binding may be attributed to the presence of RyR1 and/or RyR2 in CA1. This result is consistent with *RyR3* being enriched in hippocampal CA1 pyramidal cells in normal mice.

Histochemical analysis of *RyR3*-deficient mice showed that there were no apparent anatomical abnormalities in the hippocampus or elsewhere in the brain (data not shown). Furthermore, no differences were observed at the electron microscopic level in brain sections, including hippocampus (data not shown).

We have confirmed by immunoblot analysis that the expression of IP_3Rs in the hippocampus was not altered in the mutant mice (IP_3R1; Figure 3A; the levels of expression of IP_3R2 and IP_3R3 were too low to evaluate). The IICR activity of microsomal fractions of the hippocampus measured by fluorescence was also unchanged (homozygote: 31.1 ± 2.7, n = 3; wild-type: 34.3 ± 2.4, n = 3; Figures 3B and 3C). Taken together, these findings suggest that there are no compensations by other types of $[Ca^{2+}]_i$ release channels in *RyR3*-deficient mice.

Neuronal Plasticity in CA1 Hippocampal Neurons

We examined CA1 LTP in *RyR3*-deficient homozygotes (−/−) and wild-type (+/+) mice (21–25 days old), because *RyR3* is particularly enriched in hippocampal CA1 pyramidal neurons (Furuichi et al., 1994; Murayama and Ogawa, 1996). When LTP was evoked using high-frequency stimulation of 100 Hz for 1 s (long tetanus), the increase in the initial slope of field excitatory postsynaptic potentials (EPSPs) was not significantly different between −/− and +/+ mice, although the increase in the −/− mice tended to be greater than in the +/+ mice (+/+ mice: 37.7% ± 8.5%, n = 7; −/− mice: 45.7% ± 6.7%, n = 10 [mean ± SEM]). With near-threshold stimulation (100 Hz for 100 ms, short tetanus), however, LTP was not induced in +/+ mice but was induced in −/− mice (+/+ mice: 4.2% ± 2.2%, n = 7; −/− mice: 18.3% ± 3.1%, n = 7; Mann-Whitney U test, $p < 0.005$; Figures 4A and 4B), suggesting that −/− mice have a decreased threshold for LTP induction without affecting the maximum LTP amplitude. This feature of facilitated LTP was further investigated by the experiment using variable numbers of short tetanus application (Figure 4C).

The input/output relationship, which reflects the efficacy of synaptic transmission, was not altered in −/−

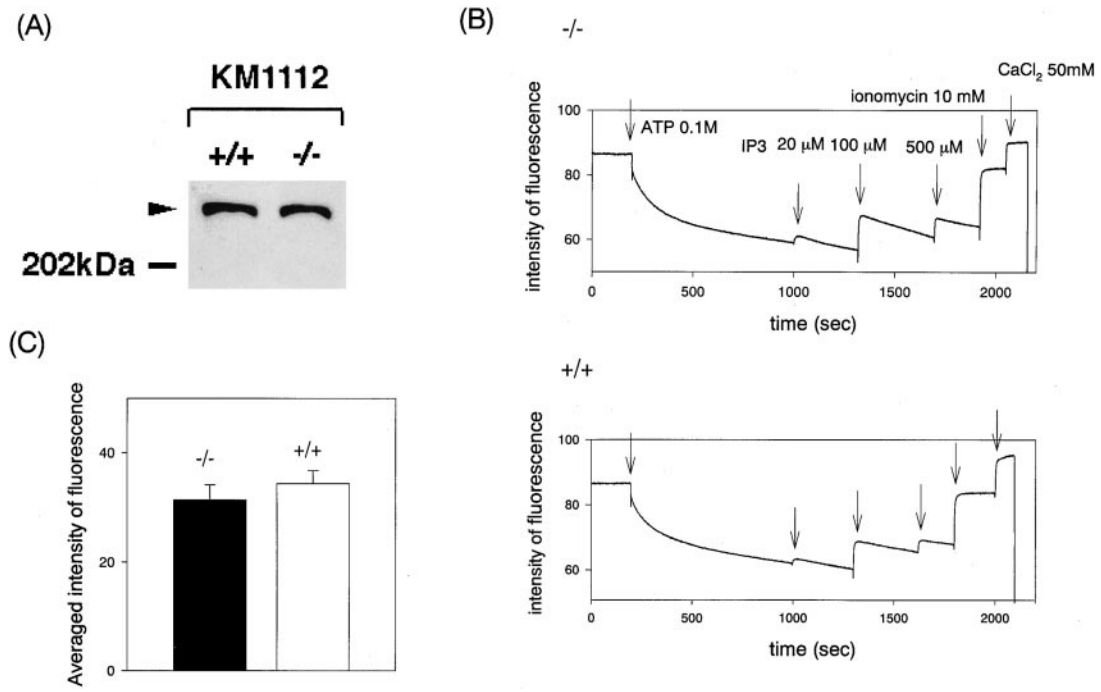

Figure 3. IP_3 Receptor Activity in *RyR3* Knockout Mouse

(A) Western blot analysis of the expression of IP_3R1 in microsomal fractions of the hippocampus. The blot was probed with KM1112, a monoclonal antibody recognizing IP_3R1.

(B and C) IICR from hippocampal microsomes of wild-type and homozygous mice. After Ca^{2+} was loaded to microsomes by applying ATP, IICR was stimulated by applying various concentrations of IP_3. The increase in the intensity of fluorescence by 100 μM IP_3 is indicated by the vertical bars (closed bars, homozygote; open bars, wild type). At the end of each recording, ionomycin and $CaCl_2$ were added to estimate the intramicrosomal Ca^{2+} content and maximum fluorescence, respectively.

mice (Figure 4D), and neither paired-pulse facilitation nor posttetanic potentiation of field EPSPs significantly differed between +/+ and −/− mice (Figures 4E and 4F). Therefore, presynaptic mechanisms that affect synaptic transmission to CA1 hippocampal neurons did not appear to be altered substantially in the *RyR3*-deficient mice.

To investigate the alterations of the basal synaptic transmission in the *RyR3* knockout mouse, miniature excitatory postsynaptic currents (EPSCs) were collected and analyzed. The frequency and amplitude of the events were not significantly different between phenotypes (frequency: −/−, 2.52 ± 0.40; +/+, 2.72 ± 0.37; amplitude: −/−, 3.32 ± 0.16; +/+, 3.04 ± 0.16; n = 5 each; Figures 5A and 5B). The amplitude of NMDA and AMPA currents at the holding potential, +40 mV, were measured and compared, and resulted in no statistical difference (−/−: NMDA, 51.2 pA; AMPA, 136.9 ± 11.7 pA; +/+: NMDA, 53.8 ± 4.09; AMPA, 134.6 ± 7.80; n = 5 each; Figure 5C). I–V curves of NMDA currents with applied voltage steps, ranging from −80 mV to +40 mV, were plotted (no significant difference, paired t test; Figure 5D). These data suggested that basal synaptic transmission and responses were not significantly altered in the *RyR3* knockout mouse.

Next, the possible NMDA receptor dependence of LTP induced by a short or long tetanus was examined (Figures 6 and 7). NMDA whole-cell currents in the mutant mouse were completely abolished in the presence of 50 μM D-AP5 (data not shown). In *RyR3*-deficient mice, a short tetanus induced LTP in the presence of 50 μM D-AP5, with a gradual increase to a stable potentiated slope of the EPSP after stimulation (+/+ mice: 1.3% ± 1.2%, n = 7; −/− mice: 23.0% ± 4.6%, n = 7; $p < 0.01$; Figures 6A and 6B). The amplitude of LTP induced by a short tetanus was similar with or without D-AP5 in *RyR3*-deficient mice. Long tetanus–induced LTP was blocked by D-AP5 in wild-type mice; however, long tetanus–induced LTP persisted in the presence of 50 μM D-AP5 in *RyR3*-deficient mice (18.7% ± 2.9%, n = 5; Figure 6B). Because a major source of Ca^{2+} influx occurs through NMDA receptors and voltage-dependent Ca^{2+} channels (VDCCs), we examined LTP induction using a short tetanus in the presence of 20 μM nimodipine, an L-type Ca^{2+} channel blocker, or 50 μM NiCl, a T-type Ca^{2+} channel blocker. Neither compound alone blocked LTP induction in *RyR3*-deficient mice (nimodipine-treated −/− mice: 19.4% ± 2.9%, n = 7; Figure 6C; NiCl-treated −/− mice: 13.6% ± 2.1%, n = 7; Figure 7A; there was no statistically significant difference between treated and untreated −/− mice); however, coapplication of 50 μM D-AP5 and 20 μM nimodipine blocked LTP in *RyR3*-deficient mice (+/+ mice: 0.7% ± 1.3%, n = 7; −/− mice: 3.9% ± 3.4%, n = 5; Figures 6C and 7D), while coapplication of 50 μM D-AP5 and 50 μM NiCl did not block LTP in *RyR3*-deficient mice (+/+ mice: 2.6% ± 1.3%, n = 7; −/− mice: 18.3% ± 1.5%, n = 5; $p < 0.01$; Figures 7A and 7D; there was no statistically significant difference between treated and untreated −/− mice). These data suggest that *RyR3*-defi-

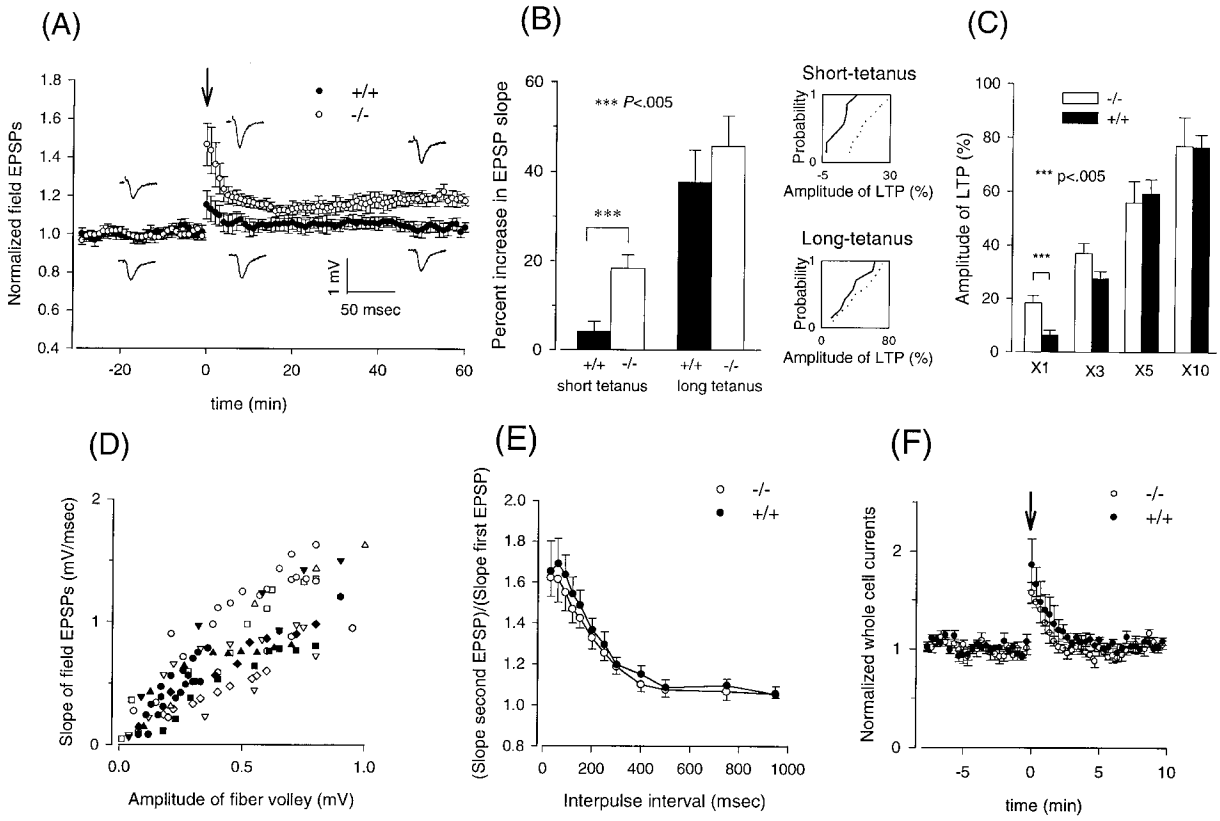

Figure 4. Hippocampal CA1 LTP in Slices from Wild-Type (+/+) and Mutant (−/−) Mice

(A) Amplitude of field EPSPs evoked by high-frequency stimulation of 100 Hz for 100 ms (short tetanus) in wild-type (closed circles; n = 9) and mutant (open circles; n = 10) mice. The amplitude of LTP was significantly higher in mutant mice compared with wild-type mice (Mann-Whitney U test, $p < 0.005$). Note the marked increase in short-term potentiation in the mutant mice. High-frequency stimulation was applied at the time indicated by the arrow. Data points represent mean ± SEM. Representative traces recorded at the three time points are included as insets. Upper traces are from mutant mice, and lower traces are from wild-type mice.

(B) Summary of LTP in wild-type mice (closed bars) and mutant mice (open bars) following short and long tetanus stimuli. The slopes of the field EPSPs, recorded 40–60 min after high-frequency stimulation, were averaged and compared to the slopes of the EPSPs recorded 20 min before the stimulation. Cumulative histogram is included as an inset (wild type, solid line; homozygote, dotted line).

(C) Multiple burst stimulation (100 Hz, 100 ms; 1–10 bursts with 10 s interburst intervals). Amplitude of LTP was measured and compared (open bars, homozygote; closed bars, wild type; n = 5 for each experiment; vertical line indicates standard error).

(D) Input/output relationship. The relationship between the amplitude of fiber volleys and the corresponding slope of field EPSPs is plotted (open symbols, −/− mice, n = 7; closed symbols, +/+ mice, n = 7).

(E) The ratio of the slope of the field EPSPs evoked by the second stimulus and that evoked by the first stimulus is plotted at various interpulse intervals (open circles, −/− mice, n = 7; closed circles, +/+ mice, n = 7). Data points represent mean ± SEM.

(F) Posttetanic potential (PTP). Whole-cell currents, recorded with the voltage clamped at −80 mV in the presence of 50 μM D-AP5, are plotted. A short tetanus was applied at the time indicated by the arrow. Although PTP tended to be suppressed further in *RyR3*-deficient mice than in the wild type, no significant differences were observed (open circles, −/− mice, n = 6; closed circles, +/+ mice, n = 6).

cient mice have a reduced threshold for both NMDA-dependent and VDCC-dependent LTP in CA1 hippocampal neurons.

Application of the mGluR antagonist (RS)-α-methyl-4-carboxyphenylglycine (MCPG; 500 μM) did not affect short tetanus–induced LTP in *RyR3*-deficient mice (+/+ mice: 2.4% ± 1.6%, n = 7; −/− mice: 19.9% ± 2.5%, n = 7; $p < 0.01$; there was no statistically significant difference between treated and untreated −/− mice); however, when coapplied with 50 μM D-AP5, MCPG completely blocked LTP (+/+ mice: 1.9% ± 1.5%, n = 5; −/− mice: 1.5% ± 1.4%, n = 6; Figures 7B and 7D). These data suggest that mGluR activity contributes to the enhancement of LTP induction by modifying channel properties or by other processes required for establishing LTP, possibly including activation of protein kinase C (Malenka et al., 1986; Bortolotto and Collingridge, 1993). To examine the possibility that excess Ca^{2+} influx through VDCCs results in L-type VDCC-dependent LTP, we measured Ca^{2+} currents under voltage clamp conditions while applying voltage in steps of 10 mV from −80 mV to +50 mV. Ca^{2+} currents evoked by these steps were not significantly altered in *RyR3*-deficient mice (at $V_H = -20$ mV, $p = 0.078$, Student's t test; Figure 7C).

We also examined another type of plasticity, LTD, in CA1 hippocampal neurons in *RyR3*-deficient mice. Administrating low-frequency stimulation to Schaffer collaterals induced LTD in wild-type mice (−14.8% ±

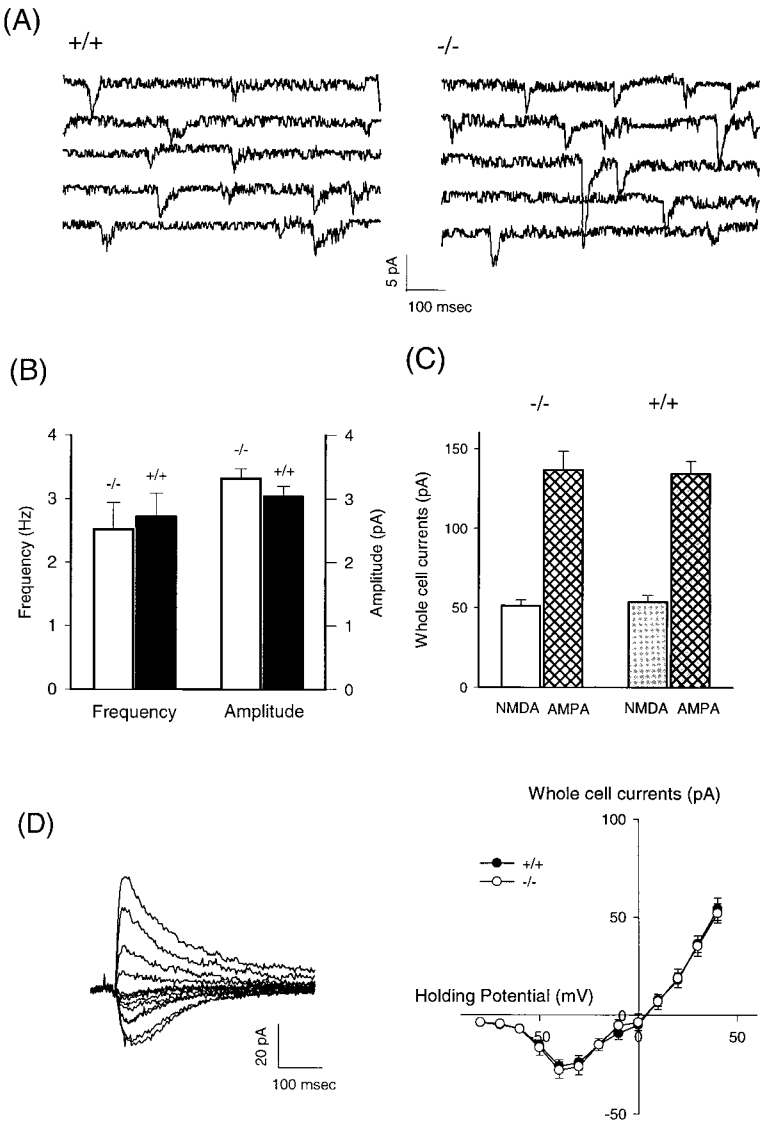

Figure 5. Basal Synaptic Transmission

(A) An example of mini-EPSCs recorded in wild-type (left) and homozygous (right) *RyR3* knockout mouse hippocampus.

(B) Neither amplitude nor frequency of mini-EPSCs was significantly different between genotypes. Each bar indicates mean ± SEM (n = 5, statistically not significant).

(C) The average of whole-cell NMDA and AMPA currents. Amplitudes of AMPA and NMDA currents were compared under membrane voltage clamp at +40 mV.

(D) At left is an example of the transsynaptic NMDA currents. NMDA currents were monitored under voltage clamp configuration. Membrane voltages were shifted from −80 to +40 mV. Scale bars are indicated in the inset. At right is the average of I–V curves of homozygous and wild-type mice (n = 5).

3.8%, n = 6) but not *RyR3*-deficient mice (+1.6% ± 2.1%, n = 6; $p < 0.01$; Figure 8).

Spatial Learning Task

We then tested *RyR3*-deficient mice for spatial learning in a Morris water maze (Figure 9). During the 7 days of training, there were no significant differences between wild-type (n = 10) and *RyR3*-deficient (n = 12) mice (male littermates, 8 weeks old) in the time taken to reach the hidden platform (escape latency; Figure 9A). In the probe trial test, however, in which the platform was removed after the training schedule described above, *RyR3*-deficient mice spent significantly more time than the wild-type mice in the quadrant where the platform had been (ANOVA $F[1,20] = 5.680$, $p = 0.0272$; Figure 9C). Furthermore, *RyR3*-deficient mice tended to cross the platform site more frequently than did the wild-type mice ($F[1,20] = 4.204$, $p = 0.0517$; Figures 9D and 9E). In a cued-platform task, a nonspatial learning task in which there was a landmark to indicate the position of the platform, the performance of wild-type and *RyR3*-deficient mice was similar (Figure 9B). This result, together with the data demonstrating that the swimming distance in the probe trial was similar for wild-type and *RyR3*-deficient mice (+/+ mice: 1685.5 ± 54.1 cm, n = 10; −/− mice: 1581.9 ± 47.2 cm, n = 12), indicates that swimming motivation and ability were not different between wild-type and *RyR3*-deficient mice. This suggests that the difference in performance of *RyR3*-deficient mice in the probe trial test was related to enhanced spatial learning. The probe trial provide a more sensitive evaluation of spatial learning (Abeliovich et al., 1993; Wu et al., 1995), because it has become apparent that mice can adopt a learning strategy other than spatial learning in the escape latency test.

Discussion

Bifunctional Effect of Increased Intracellular Ca^{2+} on LTP Induction in Hippocampal Neurons

In the present study, we observed an enhancement of LTP induction in hippocampal CA1 pyramidal cells of *RyR3*-deficient mice. This suggests, in contrast to the excitatory role of Ca^{2+} influx through NMDA and VDCC channels, *RyR3*-mediated Ca^{2+} release from internal

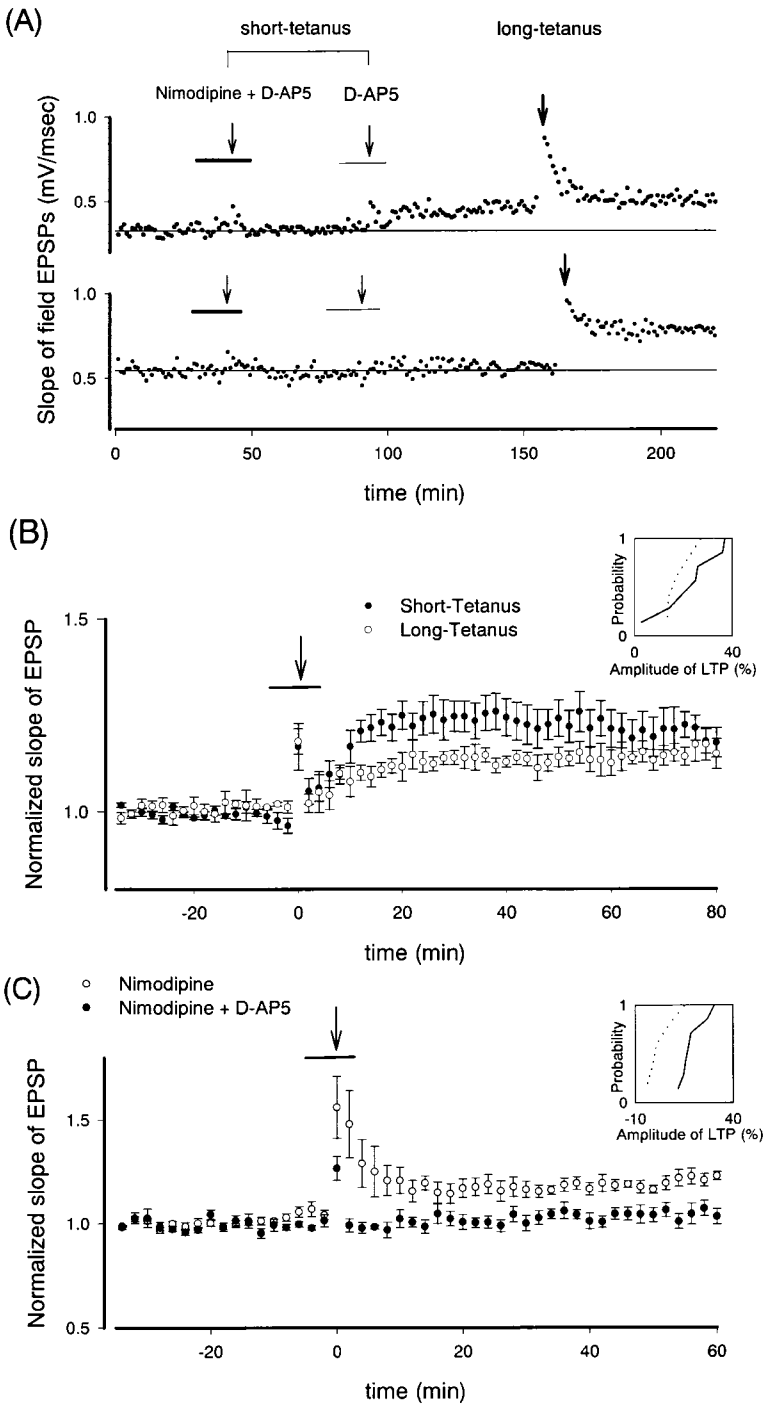

Figure 6. NMDA-Independent LTP Induction in Mutant Mice

(A) Representative traces showing the effects of an NMDA antagonist and an L-type VDCC antagonist on LTP induced by short and long tetanus stimuli (upper trace, −/− mice; lower trace, +/+ mice). Simultaneous application (thick solid bars) of 50 μM D-AP5, an NMDA-receptor antagonist, and 20 μM nimodipine, an L-type VDCC blocker, inhibited LTP induced by short tetanus stimuli. The application of 50 μM D-AP5 alone (thin closed bars) with short tetanus stimuli induced LTP in *RyR3*-deficient mice but not in wild-type mice. Tetanic stimuli were applied at the times indicated by thin arrows (short tetanus) and thick arrows (long tetanus).

(B) The effects of 50 μM D-AP5 on short tetanus–induced LTP (closed circles) and long tetanus–induced LTP (open circles) in *RyR3*-deficient mice. Data points represent mean ± SEM. Data was normalized to the averaged EPSPs for 20 min directly prior to D-AP5 application. Cumulative histogram is included as an inset (short tetanus, solid line; long tetanus, dotted line).

(C) The effects of 20 μM nimodipine alone (open circles) and the coapplication of 20 μM nimodipine (bar) and 50 μM D-AP5 (closed circles) on short tetanus-induced (arrow) LTP in *RyR3*-deficient mice. The time during which the drugs were applied is indicated by the closed bar, and a short tetanus was applied at the time indicated by the arrow. Data points represent mean ± SEM. Cumulative histogram is included as an inset (nimodipine, solid line; nimodipine + D-AP5, dotted line).

stores suppresses the induction of LTP. Interestingly, a similar enhancement of LTP induction in hippocampal CA1 neurons was observed in IP_3R1 knockout mice (Kato et al., 1997, Soc. Neurosci., abstract). Together, these results suggest that regardless of its source, release of Ca^{2+} from intracellular stores has a suppressive effect on the induction of hippocampal LTP.

The results of pharmacological studies examining the role of RyRs in synaptic plasticity are controversial (Obenaus et al., 1989; O'Mara et al., 1995; Wang et al., 1996). In the rodent cerebellum, however, IICR and CICR are required for the induction of LTD (Kohda et al., 1995; Inoue et al., 1998), which is thought to be involved in motor coordination. In particular, IP_3R1 and RyR1 are predominantly expressed in the cerebellum, suggesting that Ca^{2+} release from those subtypes of receptors is significant for cerebellar function.

NMDA-Independent LTP Induction

The enhancement of L-type VDCC activation by RyRs has been reported (Chavis et al., 1996; Nakai et al., 1996) in myotubes and cerebellar granule cells. It has been suggested that RyRs modulate VDCC activity indirectly via excitatory feedback in these cells. In hippocampal

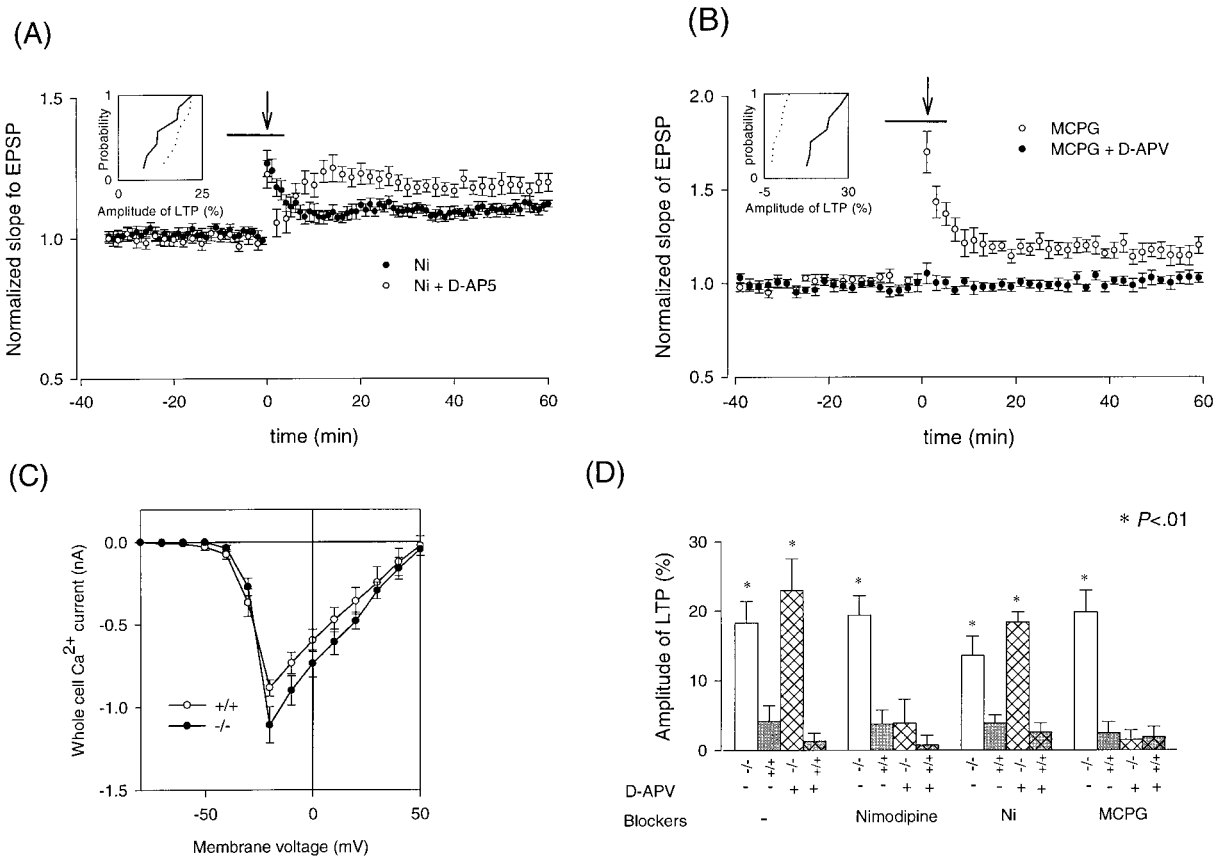

Figure 7. Effect of Various Blockers on NMDA-Independent LTP

(A) The effects of 20 mM NiCl alone (closed circles), and the coapplication of 20 mM NiCl and 50 μM D-AP5 (open circles) on short tetanus–induced (arrow) LTP in *RyR3*-deficient mice. The time during which the drugs were applied is indicated by the solid bar, and a short tetanus was applied at the time indicated by the arrow. Data points represent mean ± SEM. Cumulative histogram is included as an inset (Ni, solid line; Ni + D-AP5, dotted line).

(B) The effects of 500 μM MCPG alone (open circles) and the coapplication of 500 μM MCPG and 50 mM D-AP5 (closed circles) on short tetanus–induced LTP in *RyR3*-deficient mice. The time during which the drugs were applied is indicated by the closed bar, and a short tetanus was applied at the time indicated by the arrow. Data points represent mean ± SEM. Cumulative histogram is included as an inset (MCPG, solid line; MCPG + D-AP5, dotted line).

(C) Ca^{2+} currents in whole-cell recordings under voltage-clamped conditions (−80 mV). Depolarizing current steps of 10 mV from −80 to +50 mV for 800 ms were applied, and the peaks of the inward currents were measured (open circles, +/+ mice, n = 8; closed circles, −/− mice, n = 10). TEA (10 mM), BAPTA (5 mM), and QX-314 (10 mM) were included in the recording pipette, and 20 mM TEA was added to the external solution in which NaCl was decreased so that osmolarity was constant.

(D) Summary of the effects of receptor or channel blockers on short tetanus–induced LTP. Each group contains four bars indicating, from left to right: −/− and +/+ without D-AP5, and −/− and +/+ with D-AP5. Data points represent mean ± SEM (Mann-Whitney U test, *p < 0.01).

CA1 neurons, however, we found that the Ca^{2+} current evoked by depolarization tended to be smaller in *RyR3*-deficient mice. Although it has been thought that there is no direct coupling between L-type VDCC and *RyR3*, it is interesting to note that inactivation of *RyR3* activity tended to decrease VDCC currents in *RyR3*-deficient mice.

The application of high-frequency stimulation to the Schaffer collaterals in *RyR3*-deficient mice induced membrane depolarization mediated by VDCCs and ionotropic glutamate receptors. Because posttetanic potentiation related to transmitter release during high-frequency stimulation did not increase in *RyR3*-deficient mice, it is likely that this membrane depolarization reflects the excitability of the postsynaptic membrane. In the present study, the membrane depolarization during high-frequency stimulation was significantly smaller (Mann Whitney U test, $p < 0.05$; data not shown), suggesting that the excitability of the postsynaptic membrane was not increased in *RyR3*-deficient mice. Therefore, the enhancement of LTP induction cannot be explained either by an increase in cell membrane excitability at either pre- or postsynaptic sites or by an increase in Ca^{2+} influx.

It is possible that mechanisms to compensate for lacked *RyR3* activity in *RyR3*-deficient mice result in the enhanced LTP observed in the present study. The most likely candidate for this mechanism is upregulation of other subtypes of RyRs, RyR1 and RyR2. We observed a significant decrease in ryanodine binding in the hippocampus with no significant changes in other parts of the brain. Together with the result of immunoblot analy-

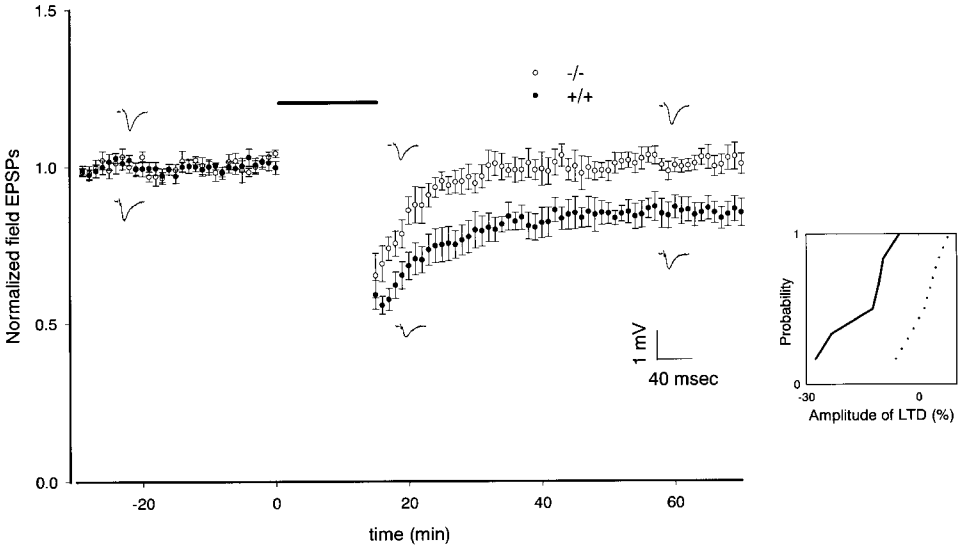

Figure 8. LTD Induction in *RyR3* Knockout Mouse

LTD induction using low-frequency stimulation (open circles, −/− mice, n = 7; closed circles, +/+ mice, n = 7; $p < 0.01$). Low-frequency stimuli were applied at the time shown as the closed bar on the panel. Cumulative histogram is included as an inset (wild type, solid line; homozygote, dotted line).

sis, we conclude that the expression of other subtypes of RyRs was unchanged in *RyR3*-deficient mice. The other possible candidate for this mechanism could be an increase in the activity of IP_3R. However, this possibility is unlikely because the Western blotting analysis and the measurement of IICR activity showed the expression and the activity of IP_3Rs was not altered in *RyR3* knockouts. Thus, it appears that neither the increase in Ca^{2+} influx nor the increase in Ca^{2+} release from ER via redundant mechanisms is responsible for the decreased threshold for LTP induction in *RyR3*-deficient mice. The most likely explanation is that a smaller increase in $[Ca^{2+}]_i$ is required for LTP induction. Ca^{2+} release triggered by activation of *RyR3* may in turn activate an inhibitory mechanism; therefore, removal of *RyR3* may disinhibit the system.

A Possible Mechanism Underlying the Bifunctional Effect of Increased Intracellular Ca^{2+}

The bifunctional role of $[Ca^{2+}]_i$ transients, which are keys in the regulation of synaptic strength, may be due to the differential activation of Ca^{2+}-sensitive target molecules. For example, both Ca^{2+}-sensitive phosphatases and kinases with varying requirements for Ca^{2+} activation have been shown to modulate LTP (Malenka, 1994; Coussens and Teyler, 1996). The regulation of synaptic plasticity by phosphatases, especially calcineurin, which is abundant in the central nervous system, is currently an area of intense interest (Mulkey et al., 1993, 1994), and it has been proposed that phosphatase activity may inhibit the protein kinase A–dependent consolidation of short- to long-term memory (Mansuy et al., 1998; Winder et al., 1998). Thus, the amplitude and kinetics of $[Ca^{2+}]_i$ transients may affect the relative balance of dephosphorylation and phosphorylation (i.e., inhibition and facilitation), possibly resulting in opposing forms of synaptic plasticity such as LTD and LTP, respectively. To explain the facilitated LTP in *RyR3*-deficient mice from the point of balance between phosphorylation and dephosphorylation, we hypothesized that decreased activity of RyRs in the CA1 region may cause less phosphatase activity. To address this issue, we examined LTD induction in hippocampal CA1, because the requirement of phosphatase activity for CA1 LTD has been well investigated. We found that LTD induction was completely eliminated in *RyR3*-deficient mice, suggesting that the phosphatase activity in these mice is decreased. Nitric oxide (NO) is another molecule that may be involved in the suppression of LTP, because the activation of NO synthase is Ca^{2+} dependent, has been reported to raise the threshold for LTP induction (Kato et al., 1993), and has also been reported to be involved in LTD induction and depotentiation in the rodent hippocampus (Gage et al., 1997; but see Cummings et al., 1994).

Modulation of NMDA-Independent LTP by Metabotropic Receptors

The decreased threshold for LTP induction in *RyR3*-deficient mice results from the smaller required increase in $[Ca^{2+}]_i$; thus, this LTP is NMDA-independent LTP. The facilitating effect of mGluR activity on this NMDA-independent LTP induction probably relates to the contribution of PKC rather than the IP_3 pathway, because we previously found that IP_3R activity suppresses LTP induction (Kato et al., 1997, Soc. Neurosci., abstract), and facilitation of LTP by activation of PKC has been well established (Malenka et al., 1986; Abeliovich et al., 1993).

Variant Role of Ca^{2+} Released via Activation of IP_3R and Other Subtypes of RyRs

Results from RyR knockout mice studies have demonstrated that release of Ca^{2+} from intracellular stores mediated by both IP_3R and RyR appears to suppress LTP in wild-type mice, raising the question of whether this

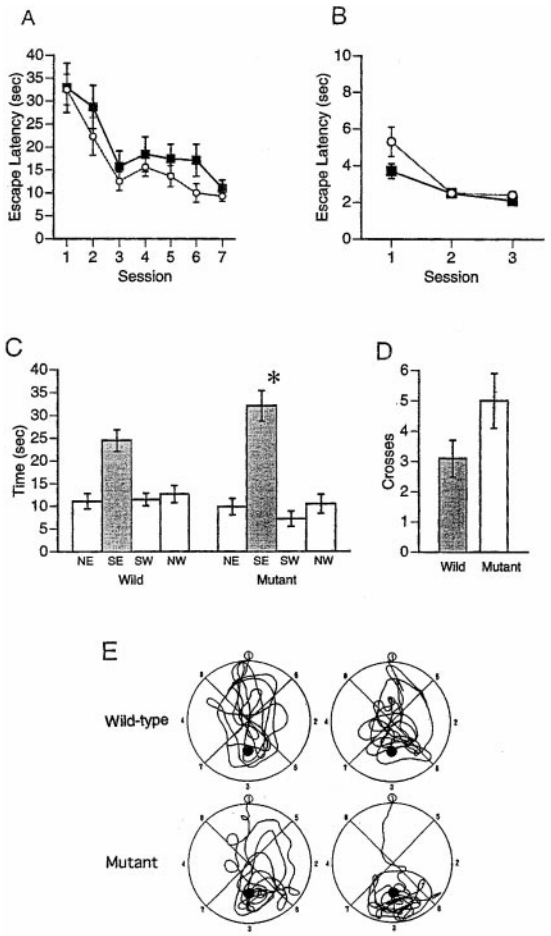

Figure 9. Spatial Learning of Wild-Type (+/+) and *RyR3*-Deficient (−/−) Mice in a Morris Water Maze

Wild-type (n = 10) and *RyR3*-deficient (n = 12) male littermates were used.

(A) Escape latencies in the hidden-platform task over seven training sessions (+/+ mice, closed squares; −/− mice, open squares). No significant difference was found between genotypes. Data points represent mean ± SEM.

(B) Escape latencies in the cued-platform task over three training sessions (+/+ mice, closed squares; −/− mice, open squares). No significant difference was found between genotypes. Data points represent mean ± SEM.

(C) Time spent in each quadrant of the water maze during the probe trial. The southeast (SE) quadrant previously contained the platform. *RyR3*-deficient mice spent significantly more time than wild-type mice in the quadrant where the platform had been (ANOVA $F[1,20] = 5.680$, $*p < 0.05$). Data points represent mean ± SEM.

(D) The number of times the former platform site was crossed during the probe trial. Data points represent mean ± SEM.

(E) The tracking traces in the probe trial. Two examples from each genotype that exhibit the average number of crossings for each group. The former platform sites are displayed as the closed circles.

effect is mediated by similar or different mechanisms. LTP induction in IP_3R1 knockout mice was found to be fully NMDA dependent (T. Nagase et al., personal communication), suggesting that the mechanism underlying this facilitation is the increase in Ca^{2+} influx through NMDA channels. In contrast, LTP induction in *RyR3*-deficient mice is NMDA independent, suggesting that the mechanism of enhancement of LTP induction differs. The difference in localization of IP_3Rs and RyRs (Nakanishi et al., 1992; Nori et al., 1993; Tse et al., 1997) may underlie their different roles in synaptic plasticity.

The next question is whether the contribution of *RyR3* and other subtypes of RyRs to synaptic plasticity differs. The results of RyR knockout mice studies previously reported suggest that the effect of *RyR3* and RyR1 activity is additive in skeletal muscle, although their characteristics are subtly different (Takeshima et al., 1996; Bertocchini et al., 1997; Ikemoto et al., 1997). Consistent with the results of the present study, the effect of exogenously applied, general RyR blockers on LTP and LTD induction suggest that the effect of *RyR3* supplements that of other subtypes of RyRs in neurons (Reyes and Stanton, 1996; Wang et al., 1996, 1997). Considering that *RyR3* has a low Ca^{2+} sensitivity (Takeshima et al., 1996), *RyR3* acts as a secondary Ca^{2+} amplifier during the large increase in $[Ca^{2+}]_i$ evoked by electrical stimulation typically used in electrophysiological experiments.

Links to Spatial Learning

Taken together, these results suggest that Ca^{2+} from different sources, such as extracellular via NMDA receptors and VDCCs or intracellular via IP_3Rs and RyRs, may have varying and different effects on LTP and spatial learning. While the exact molecular mechanisms underlying these effects are not known, the relative level of phosphorylation determined by phosphatases and kinases activated by different levels of $[Ca^{2+}]_i$ and by increases in $[Ca^{2+}]_i$ from different sources is an attractive candidate. The causal links between the enhancement of LTP and improvement of spatial learning are not obvious; however, the decrease in ryanodine binding in the central nervous system, especially in the hippocampal CA1 neurons, resulted in enhancement of LTP induction and improvement in the probe trial test, supporting the hypothesis that the hippocampus is a critical region for memory formation (Morris et al., 1986; Diana et al., 1995; Tsien et al., 1996).

Experimental Procedures

Targeting Vector Construction and Generation of *RyR3*-Deficient Mice

A mouse *RyR3* genomic fragment (982 bp) was amplified by a set of primers corresponding to nucleotide positions between 852 and 994 of the rabbit *RyR3* cDNA. Using this fragment as a probe, genomic clones containing five exons (corresponding to exons 4–8 of human RyR1) and the flanking introns of the *RyR3* gene were isolated from 129/SvJ mouse λ genomic library (Stratagene). The fragments used to construct the targeting vector were a 4.4 kb EcoRV–EcoRV fragment 5′ to exon 6, a 5.0 kb EcoRV–SalI fragment (The SalI site was derived from a lambda FIX II vector [Stratagene]) 3′ to exon 7, a 1.8 kb PGK-*neo* gene cassette derived from pKJ1 (McBurney et al., 1991; a gift from Michael A. Rudnicki), and a 1.0 kb XhoI–SalI diphtheria toxin A fragment (*DT-A*) gene cassette derived from pMC1DT-A (Yagi et al., 1990; a gift from Shinichi Aizawa; Figure 1). Thus, a 0.85 kb EcoRV–EcoRV fragment containing parts of exon 6 and exon 7 was replaced by a 1.8 kb PGK-*neo* gene cassette as a positive selection marker carrying stop codons in all the reading frames and a poly(A) tail. A *DT-A* gene cassette was inserted downstream of exon 8 as a negative selection marker. The vector DNA was linearized with NotI and transfected into E14 ES cells (Hooper et al., 1987) by electroporation (Bio-Rad Gene Pulser set at 800 V and 3 μF). G418 (150 μg/ml) -resistant clones (384) were screened by digestion of the genomic DNA with EcoRI and hybridization with

a 0.6 kb EcoRI–EcoRV fragment as a 5′ external probe. The wild-type allele gave rise to a 7.5 kb fragment, and the mutant allele gave rise to a 5.0 kb fragment (Figure 1A). The desired homologous recombination 3′ to the disrupted region was also confirmed with the *neo* probe (data not shown). Six ES clones were determined to be positive for the desired recombination. Chimeric mice were generated as described previously (Bradley, 1987). ES cells from five clones were microinjected into C57BL/6J blastocysts at 3.5 days postcoitum, and the embryos were transferred into the uteri of pseudopregnant ICR mice. Two clones gave rise to germline chimeras. Mice heterozygous for the mutation were obtained by cross-breeding the chimeras with C57BL/6J mice. The heterozygotes were further crossbred with C57BL/6J mice two to six times, and the resultant heterozygotes were interbred to obtain the littermate wild-type and homozygous mice that were used in the present study. The genotypes of the mice were determined by Southern blot analysis of genomic DNA prepared from tail tissue (Figure 1B).

Antibodies and Western Blots

B4 peptide, Lys-2693 to Gln-2712 of rabbit *RyR3* (KEGEALVQLRENEKIRSVSQ), was synthesized using a 430A peptide synthesizer (Applied Biosystems) and purified by reverse-phase high-performance liquid chromatography. Polyclonal rabbit sera were raised against B4 peptide conjugated to keyhole limpet hemocyanin. Immunoglobulins were precipitated from the sera using 33% ammonium sulfate, and the antibody was further purified by affinity chromatography with agarose gel (Affigel 10; Bio-Rad) conjugated with the B4 peptide. This anti-B4 antibody was confirmed to be *RyR3* specific, and cross-reactivity with RyR1 and RyR2 was not observed (data not shown). The anti-C2 antibody was prepared as previously described (Kuwajima et al., 1992).

The cerebrum, including the hippocampus, was homogenized in a solution containing 0.32 M sucrose, 5 mM Tris–HCl (pH 7.4), 1 mM EDTA, 0.1 mM PMSF, 10 μM leupeptin, 10 μM pepstatin A, and 1 mM 2-mercaptoethanol (homogenizing buffer) and was centrifuged for 5 min at 1000 × g at 4°C. The supernatant was centrifuged for 60 min at 100,000 × g at 2°C, and the pellet was homogenized in a homogenizing buffer. This solution was centrifuged for 60 min at 20,000 × g at 2°C, and the supernatant was again centrifuged for 60 min at 100,000 × g at 2°C. The pellet (microsomal fraction) was resuspended in a homogenizing solution and the protein concentration was measured using a Bio-Rad protein assay kit. The samples (5 μg) were applied to SDS–PAGE gels and detected by Western blot probed with anti-B4 or anti-C2 antibody and then probed with biotinylated anti-rabbit immunoglobulin G antibody. The signal was amplified using a Vectastain Elite ABC Kit (Vector), and peroxidase-coupled detection was carried out using the enzyme-linked chemiluminescence method with an ECL kit (Amersham). Detection of IP_3Rs by subtype-specific monoclonal antibodies was done as described previously (Sugiyama et al., 1994).

Measurement of IP_3-Induced Ca^{2+} Release from Microsomes

Changes in Ca^{2+} concentration were monitored by measuring fluorescence of Ca^{2+} Green 1 using a luminescence spectrometer (Perkin Elmer LBS50B). Hippocampal microsomes (180 μg) were diluted to 450 μl with Ca^{2+}-releasing buffer, supplemented with phosphocreatine, creatine kinase, DTT, and oligomycin to a final concentration of 10 mM, 40 U/ml, 1 mM, and 2.5 μg/ml, respectively. Ca^{2+} loading to microsomes was initiated by adding 0.1 M ATP. After 1000 s, Ca^{2+} release was triggered by the addition of various amounts of IP_3. Before ending the experiment, 10 mM ionomycin was added to estimate intramicrosomal Ca^{2+} content, and 50 mM $CaCl_2$ to get R_{max} and F_{max}.

[^{3}H]Ryanodine Binding to Brain Sections and Data Analysis

[^{3}H]Ryanodine binding to brain sections was performed essentially according to the methods of Padua et al. (1991). Coronal cryosections 20 μm in thickness were prepared from frozen brains of wild-type (+/+) and *RyR3*-deficient (−/−) mice (P25–P29). Sections at the hippocampus–thalamus level were preincubated twice in buffer A (20 mM PIPES–KOH [pH 8.0], 1.0 M KCl, 550 mM ATP, 100 mM $CaCl_2$, and 1.0 mM PMSF) for 15 min each and then incubated with 15 nM [^{3}H]ryanodine (specific activity = 68.3 Ci/mmol; NEN Research Products/DuPont) in the same buffer for 15 min at room temperature. The reactions were terminated by a subsequent 5 min wash in ice-cold buffer A, followed by a second 5 min wash in buffer A diluted 1:10 (v/v) with distilled water. The sections were then rinsed in ice-cold distilled water for 5 min, dried, and exposed to Ultrofilm[^{3}H] (Leica Instruments) with calibrated ^{3}H-embedded polymer standard for 5 weeks at 4°C. Nonspecific binding was determined by parallel incubation in the presence of 15 mM unlabeled ryanodine. The autoradiographic results were analyzed using a computerized digital image processing system as described (Tanaka et al., 1988, 1991).

Electrophysiology

Hippocampal slices were prepared from mice lacking *RyR3* (21–25 days old). Mice were anesthetized with ether and decapitated. Hippocampi were dissected rapidly and transverse slices (500 μm thick) were cut using a rotary tissue slicer at room temperature and then maintained in an incubation chamber in the presence of gassed (95% O_2/5% CO_2) extracellular solution containing (in mM): 124 NaCl, 3.0 KCl, 2.0 $CaCl_2$, 2.0 $MgSO_4$, 1.25 $NaHCO_3$, and 10 glucose for at least 2 hr at 30°C. Immediately prior to each experiment, individual slices were transferred to a submersion recording chamber, where they were superfused continuously with extracellular solution (~3 ml min^{-1}) at 30°C. Field recordings were obtained from the apical dendritic region of the CA1 pyramidal cells using glass microelectrodes (3–8 MΩ) filled with 2 M NaCl. The Schaffer collateral–commissural fibers were stimulated every 20 s in the stratum radiatum using a bipolar electrode and 0.3 ms constant-current pulses at an intensity sufficient to evoke a 30% maximal response. LTP was produced by an electrical high-frequency stimulation (100 Hz for 1 s or 0.1 s) administered using the same stimulus intensity. LTD was induced by electrical low-frequency stimulation (1 Hz, 15 min). The amplitude of LTP and LTD was calculated as the ratio of the averaged stable responses after the induction (usually 40–60 min) to the control responses just before the induction (averaged for 20 min). The responses of CA1 neurons were recorded using the "blind" whole-cell clamp method using an Axopatch-200B amplifier (Axon Instruments). Pipettes were routinely filled with solution containing (in mM): 130 cesium methanesulfonate, 10 tetraethylammonium chloride (TEA), 5 NaCl, 1,2-bis(2-aminophenoxy)ethane-N,N,N′, N′-tetraacetic acid (BAPTA), and 10 HEPES with pH adjusted to 7.3 using CsOH. ATP (2 mM) and GTP (0.3 mM) were also included in the pipette solution. Voltage clamp currents were filtered at 2 kHz and were digitized at 5 kHz using a microcomputer data acquisition system. Responses to paired stimuli (30–950 ms interpulse intervals) of field EPSPs of the CA1 area were recorded, and the ratio of the initial slope of the second pulse to that of the first pulse was calculated. Posttetanic potentiation was recorded using whole-cell patch clamp under voltage clamp at −80 mV by applying a short tetanus in the presence of 50 μM D-AP5. BAPTA in the recording pipette was increased to 5 mM to minimize the effect of postsynaptic Ca^{2+} on the evoked potential. NMDA currents were monitored in the presence of 20 μM 6-cyano-7-nitroquinoxaline-2,3-dione (CNQX) and 20 μM bicuculline. AMPA currents were monitored in the presence of 20 μM bicuculline and 50 μM D-AP5. Miniature EPSCs were obtained under the voltage clamp configuration at −80 mV in the presence of 1 μM TTX and 20 μM bicuculline. The peak amplitude larger than 2 pA has been counted as an event. Several slices were obtained from one animal, and each slice was used for a different kind of experiment.

Spatial Learning Test

All behavioral tests were conducted between 9 a.m. and 12 a.m. in a temperature-controlled (23°C–24°C) room. The genotype of the mice was always unknown to the experimenter. Spatial learning was assessed by three variants of the Morris water maze task (Morris, 1984) adapted for mice. The maze was a 150 cm white plastic pool filled to a depth of 31 cm with 23°C–25°C water. One-way or two-way ANOVAs with repeated measures were used for statistical analysis. The three tasks were as follows.

Hidden-Platform Task

A circular, transparent acrylic platform (diameter 12 cm) was submerged 1 cm below the surface of the water in the southeast quadrant throughout the hidden-platform task. A mouse was placed in

the water facing the wall of the pool, but not touching it. If the mouse found the platform within 60 s, it was allowed to stay there for 30 s. Mice that failed to find the platform in 60 s were manually placed on the platform and they remained on it for 30 s. Each mouse was subjected to four trials per day over 7 days. There were four starting points located at the center of each quadrant, and a different starting point was used in each of the four trials. The time taken to reach the platform (escape latency) was monitored.

Probe Trial

A single probe trial was carried out after the hidden-platform training had been completed. In this trial, the platform was removed and the movement of each mouse in the pool was monitored using a computer-based video tracking system (BTA-2, Muromachi Kikai Company, Tokyo, Japan). Each mouse was placed in the pool from the northwest position and was allowed to swim for 60 s. Swimming path length, the number of times the platform site was crossed, and the time spent in the training (southeast) quadrant were recorded.

Cued-Platform Task

Cued-platform task trials began 1 day after the probe trial and consisted of four trials per day for 3 consecutive days. In this task, the platform was made visible by attaching a blackboard (9 × 19 cm) to the platform. The location of the platform varied among four possible places for each of the four daily trials. The mouse was always started at the east point and was allowed 60 s to locate the platform. If the mouse found the platform, it was allowed to stay there for 30 s. If the mouse failed to find the platform, it was placed on the platform and remained there for 30 s.

Acknowledgments

This work was supported in part by a Grant for Cooperative Research (A. F. and K. M.) from Senri Life Science Foundation and a Grant (H. O.) from the Japanese Ministry of Education, Science, Sports, and Culture of Japan. We thank Dr. H. Takeshima for providing us with the cDNA sequence of the rabbit *RyR3*; Dr. M. L. Hooper for providing E14 cells; and Drs. M. Matsumoto, M.-M. Poo, M. Nishiyama, Q. S. Hong., B. Berninger, and H. Bito for their critical reading of the manuscript. R. Ando, T. Nakayama, M. Ishiwata, and S. Fujiwara provided excellent technical assistance, and A. Hoshino and M. Saito provided animal care. We also are grateful to Drs. Y. Hinuma, M. Hatanaka, and T. Kitamura for continuous encouragement and support. All animals were treated ethically according to the rules of the Shionogi Animal Use and Care Committee.

Received April 6, 1999; revised September 24, 1999.

References

Abeliovich, A., Chen, C., Goda, Y., Silva, A.J., Stevens, C.F., and Tonegawa, S. (1993). Modified hippocampal long-term potentiation in PKCγ-mutant mice. Cell *75*, 1253–1262.

Barria, A., Muller, D., Derkach, V., Griffith, L.C., and Soderling, T.R. (1997). Regulatory phosphorylation of AMPA-type glutamate receptors by CaM-KII during long-term potentiation. Science *276*, 2042–2045.

Bertocchini, F., Ovitt, C.E., Conti, A., Barone, V., Scholer, H.R., Bottinelli, R., Reggiani, C., and Sorrentino, V. (1997). Requirement for the ryanodine receptor type 3 for efficient contraction in neonatal skeletal muscles. EMBO J. *16*, 6956–6963.

Bliss, T.V., and Collingridge, G.L. (1993). A synaptic model of memory: long-term potentiation in the hippocampus. Nature *361*, 31–39.

Bortolotto, Z.A., and Collingridge, G.L. (1993). Characterisation of LTP induced by the activation of glutamate metabotropic receptors in area CA1 of the hippocampus. Neuropharmacology *32*, 1–9.

Bradley, A. (1987). Production and analysis of chimeric mice. In Teratocarcinomas and Embryonic Stem Cells: A Practical Approach, E.J. Robertson, ed. (Oxford: IRL press), pp. 113–151.

Chavis, P., Fagni, L., Lansman, J.B., and Bockaert, J. (1996). Functional coupling between ryanodine receptors and L-type calcium channels in neurons. Nature *382*, 719–722.

Collingridge, G. (1987). Synaptic plasticity. The role of NMDA receptors in learning and memory. Nature *330*, 604–605.

Coussens, C.M., and Teyler, T.J. (1996). Protein kinase and phosphatase activity regulate the form of synaptic plasticity expressed. Synapse *24*, 97–103.

Cummings, J.A., Nicola, S.M., and Malenka, R.C. (1994). Induction in the rat hippocampus of long-term potentiation (LTP) and long-term depression (LTD) in the presence of a nitric oxide synthase inhibitor. Neurosci. Lett. *176*, 110–114.

Cummings, J.A., Mulkey, R.M., Nicoll, R.A., and Malenka, R.C. (1996). Ca^{2+} signaling requirements for long-term depression in the hippocampus. Neuron *16*, 825–833.

Diana, G., Domenici, M.R., Scotti de Carolis, A., Loizzo, A., and Sagratella, S. (1995). Reduced hippocampal CA1 Ca(2+)-induced long-term potentiation is associated with age-dependent impairment of spatial learning. Brain Res. *686*, 107–110.

Dudek, S.M., and Bear, M.F. (1992). Homosynaptic long-term depression in area CA1 of hippocampus and effects of N-methyl-D-aspartate receptor blockade. Proc. Natl. Acad. Sci. USA *89*, 4363–4367.

Ellisman, M.H., Deerinck, T.J., Ouyang, Y., Beck, C.F., Tanksley, S.J., Walton, P.D., Airey, J.A., and Sutko, J.L. (1990). Identification and localization of ryanodine binding proteins in the avian central nervous system. Neuron *5*, 135–146.

Furuichi, T., Furutama, D., Hakamata, Y., Nakai, J., Takeshima, H., and Mikoshiba, K. (1994). Multiple types of ryanodine receptor/Ca^{2+} release channels are differentially expressed in rabbit brain. J. Neurosci. *14*, 4794–4805.

Gage, A.T., Reyes, M., and Stanton, P.K. (1997). Nitric-oxide-guanylyl-cyclase-dependent and -independent components of multiple forms of long-term synaptic depression. Hippocampus *7*, 286–295.

Giannini, G., Conti, A., Mammarella, S., Scrobogna, M., and Sorrentino, V. (1995). The ryanodine receptor/calcium channel genes are widely and differentially expressed in murine brain and peripheral tissues. J. Cell Biol. *128*, 893–904.

Grover, L.M., and Teyler, T.J. (1990). Two components of long-term potentiation induced by different patterns of afferent activation. Nature *347*, 477–479.

Harvey, J., and Collingridge, G.L. (1992). Thapsigargin blocks the induction of long-term potentiation in rat hippocampal slices. Neurosci. Lett. *139*, 197–200.

Hooper, M., Hardy, K., Handyside, A., Hunter, S., and Monk, M. (1987). HPRT-deficient (Lesch-Nyhan) mouse embryos derived from germline colonization by cultured cells. Nature *326*, 292–295.

Ikemoto, T., Komazaki, S., Takeshima, H., Nishi, M., Noda, T., Iino, M., and Endo, M. (1997). Functional and morphological features of skeletal muscle from mutant mice lacking both type 1 and type 3 ryanodine receptors. J. Physiol. *501*, 305–312.

Inoue, T., Kato, K., Kohda, K., and Mikoshiba, K. (1998). Type 1 inositol 1,4,5-trisphosphate receptor is required for induction of long-term depression in cerebellar Purkinje neurons. J. Neurosci. *18*, 5366–5373.

Jia, Z., Agopyan, N., Miu, P., Xiong, Z., Henderson, J., Gerlai, R., Taverna, F.A., Velumian, A., MacDonald, J., Carlen, P., et al. (1996). Enhanced LTP in mice deficient in the AMPA receptor GluR2. Neuron *17*, 945–956.

Kato, K., Clifford, D.B., and Zorumski, C.F. (1993). Long-term potentiation during whole-cell recording in rat hippocampal slices. Neuroscience *53*, 39–47.

Kohda, K., Inoue, T., and Mikoshiba, K. (1995). Ca^{2+} release from Ca^{2+} stores, particularly from ryanodine-sensitive Ca^{2+} stores, is required for the induction of LTD in cultured cerebellar Purkinje cells. J. Neurophysiol. *74*, 2184–2188.

Kuwajima, G., Futatsugi, A., Niinobe, M., Nakanishi, S., and Mikoshiba, K. (1992). Two types of ryanodine receptors in mouse brain: skeletal muscle type exclusively in Purkinje cells and cardiac muscle type in various neurons. Neuron *9*, 1133–1142.

Lynch, G., Larson, J., Kelso, S., Barrionuevo, G., and Schottler, F. (1983). Intracellular injections of EGTA block induction of hippocampal long-term potentiation. Nature *305*, 719–721.

Malenka, R.C. (1994). Synaptic plasticity in the hippocampus: LTP and LTD. Cell *78*, 535–538.

Malenka, R.C., Madison, D.V., and Nicoll, R.A. (1986). Potentiation of synaptic transmission in the hippocampus by phorbol esters. Nature *321*, 175–177.

Mansour, S.L., Thomas, K.R., and Capecchi, M.R. (1988). Disruption of the proto-oncogene int-2 in mouse embryo-derived stem cells: a general strategy for targeting mutations to nonselectable genes. Nature *336*, 348–352.

Mansuy, I.M., Mayford, M., Jacob, B., Kandel, E.R., and Bach, M.E. (1998). Restricted and regulated overexpression reveals calcineurin as a key component in the transition from short-term to long-term memory. Cell *92*, 39–49.

McBurney, M.W., Sutherland, L.C., Adra, C.N., Leclair, B., Rudnicki, M.A., and Jardine, K. (1991). The mouse Pgk-1 gene promoter contains an upstream activator sequence. Nucleic Acids Res. *19*, 5755–5761.

McHugh, T.J., Blum, K.I., Tsien, J.Z., Tonegawa, S., and Wilson, M.A. (1996). Impaired hippocampal representation of space in CA1-specific NMDAR1 knockout mice. Cell *87*, 1339–1349.

Morris, R. (1984). Developments of a water-maze procedure for studying spatial learning in the rat. J. Neurosci. Methods *11*, 47–60.

Morris, R.G., Anderson, E., Lynch, G.S., and Baudry, M. (1986). Selective impairment of learning and blockade of long-term potentiation by an N-methyl-D-aspartate receptor antagonist, AP5. Nature *319*, 774–776.

Mulkey, R.M., and Malenka, R.C. (1992). Mechanisms underlying induction of homosynaptic long-term depression in area CA1 of the hippocampus. Neuron *9*, 967–975.

Mulkey, R.M., Herron, C.E., and Malenka, R.C. (1993). An essential role for protein phosphatases in hippocampal long-term depression. Science *261*, 1051–1055.

Mulkey, R.M., Endo, S., Shenolikar, S., and Malenka, R.C. (1994). Involvement of a calcineurin/inhibitor-1 phosphatase cascade in hippocampal long-term depression. Nature *369*, 486–488.

Murayama, T., and Ogawa, Y. (1996). Properties of Ryr3 ryanodine receptor isoform in mammalian brain. J. Biol. Chem. *271*, 5079–5084.

Nakai, J., Dirksen, R.T., Nguyen, H.T., Pessah, I.N., Beam, K.G., and Allen, P.D. (1996). Enhanced dihydropyridine receptor channel activity in the presence of ryanodine receptor. Nature *380*, 72–75.

Nakanishi, S., Kuwajima, G., and Mikoshiba, K. (1992). Immunohistochemical localization of ryanodine receptors in mouse central nervous system. Neurosci. Res. *15*, 130–142.

Nori, A., Villa, A., Podini, P., Witcher, D.R., and Volpe, P. (1993). Intracellular Ca^{2+} stores of rat cerebellum: heterogeneity within and distinction from endoplasmic reticulum. Biochem. J. *291*, 199–204.

Obenaus, A., Mody, I., and Baimbridge, K.G. (1989). Dantrolene-Na (Dantrium) blocks induction of long-term potentiation in hippocampal slices. Neurosci. Lett. *98*, 172–178.

O'Mara, S.M., Rowan, M.J., and Anwyl, R. (1995). Dantrolene inhibits long-term depression and depotentiation of synaptic transmission in the rat dentate gyrus. Neuroscience *68*, 621–624.

Ouyang, Y., Deerinck, T.J., Walton, P.D., Airey, J.A., Sutko, J.L., and Ellisman, M.H. (1993). Distribution of ryanodine receptors in the chicken central nervous system. Brain Res. *620*, 269–280.

Padua, R.A., Wan, W.H., Nagy, J.I., and Geiger, J.D. (1991). [^{3}H]ryanodine binding sites in rat brain demonstrated by membrane binding and autoradiography. Brain Res. *542*, 135–140.

Phillips, M.S., Fujii, J., Khanna, V.K., DeLeon, S., Yokobata, K., de Jong, P.J., and MacLennan, D.H. (1996). The structural organization of the human skeletal muscle ryanodine receptor (RYR1) gene. Genomics *34*, 24–41.

Reyes, M., and Stanton, P.K. (1996). Induction of hippocampal long-term depression requires release of Ca^{2+} from separate presynaptic and postsynaptic intracellular stores. J. Neurosci. *16*, 5951–5960.

Sugiyama, T., Furuya, A., Monkawa, T., Yamamoto-Hino, M., Satoh, S., Ohmori, K., Miyawaki, A., Hanai, N., Mikoshiba, K., and Hasegawa, M. (1994). Monoclonal antibodies distinctively recognizing the subtypes of inositol 1,4,5-trisphosphate receptor: application to the studies on inflammatory cells. FEBS Lett. *354*, 149–154.

Takeshima, H., Ikemoto, T., Nishi, M., Nishiyama, N., Shimuta, M., Sugitani, Y., Kuno, J., Saito, I., Saito, H., Endo, M., Iino, M., and Noda, T. (1996). Generation and characterization of mutant mice lacking ryanodine receptor type 3. J. Biol. Chem. *271*, 19649–19652.

Tanaka, K., Gotoh, F., Ishihara, N., Gomi, S., Takashima, S., and Mihara, B. (1988). Autoradiographic analysis of second-messenger systems in the gerbil brain. Brain Res. Bull. *21*, 693–700.

Tanaka, K., Gotoh, F., Gomi, S., Takashima, S., and Mihara, B. (1991). Autoradiographic analysis on second-messenger systems and local cerebral blood flow in ischemic gerbil brain. J. Cereb. Blood Flow Metabol. *11*, 283–291.

Tse, F.W., Tse, A., Hille, B., Horstmann, H., and Almers, W. (1997). Local Ca^{2+} release from internal stores controls exocytosis in pituitary gonadotrophs. Neuron *18*, 121–132.

Tsien, J.Z., Huerta, P.T., and Tonegawa, S. (1996). The essential role of hippocampal CA1 NMDA receptor–dependent synaptic plasticity in spatial memory. Cell *87*, 1327–1338.

Wang, Y., Wu, J., Rowan, M.J., and Anwyl, R. (1996). Ryanodine produces a low frequency stimulation–induced NMDA receptor–independent long-term potentiation in the rat dentate gyrus in vitro. J. Physiol. *495*, 755–767.

Wang, Y., Rowan, M.J., and Anwyl, R. (1997). Induction of LTD in the dentate gyrus in vitro is NMDA receptor independent, but dependent on Ca^{2+} influx via low-voltage-activated Ca^{2+} channels and release of Ca^{2+} from intracellular stores. J. Neurophysiol. *77*, 812–825.

Winder, D.G., Mansuy, I.M., Osman, M., Moallem, T.M., and Kandel, E.R. (1998). Genetic and pharmacological evidence for a novel, intermediate phase of long-term potentiation suppressed by calcineurin. Cell *92*, 25–37.

Wu, Z.L., Thomas, S.A., Villacres, E.C., Xia, Z., Simmons, M.L., Chavkin, C., Palmiter, R.D., and Storm, D.R. (1995). Altered behavior and long-term potentiation in type I adenylyl cyclase mutant mice. Proc. Natl. Acad. Sci. USA *92*, 220–224.

Yagi, T., Ikawa, Y., Yoshida, K., Shigetani, Y., Takeda, N., Mabuchi, I., Yamamoto, T., and Aizawa, S. (1990). Homologous recombination at c-fyn locus of mouse embryonic stem cells with use of diphtheria toxin A-fragment gene in negative selection. Proc. Natl. Acad. Sci. USA *87*, 9918–9922.